18th NORTH SEA FLOW MEASUREMENT WORKSHOP 2000

CORRECTION OF READINGS FROM AN ORIFICE PLATE INSTALLED IN REVERSE ORIENTATION

G J Brown, M J Reader-Harris and J J Gibson
National Engineering Laboratory, UK

G J Stobie, Phillips Petroleum Co UK Ltd

The accidental reversal of an orifice plate that has a bevelled downstream edge can result in a significant mismeasurement. This can occur very easily and has probably happened much more frequently than has been observed or reported.

This paper summarised work carried out by NEL to evaluate the magnitude of mismeasurement in one specific case of an orifice plate being reversed. The plate in question was installed in one of the 10-inch metering streams on the Judy platform.

A number of different methods were applied to obtain an estimate of the increase in discharge coefficient. Experimental data were replotted and extrapolated, computational fluid dynamics (CFD) was applied, and a loss-balance calculation was performed using before and after flow data and knowledge of the meter station layout. Finally a flow verification trial was conducted offshore using two live metering streams and reversing the orifice plate in one for a period of seven hours.

Taking the results together the increase in the discharge coefficient was estimated to be 22 % ± 3 %. This is equivalent to using a correction factor of 1.22 to multiply any flow derived results such as volume at standard conditions.

Further work is required before a general model can be developed to allow calculation of the change in discharge coefficient for a given plate geometry. In particular there is a need for more laboratory data from a wider range of plates.

NOMENCLATURE

A_2	Area of orifice	(m^2)
b	Bevel-width (= E-e)	(m)
C	Coefficient of discharge	
d	Diameter of orifice	(m)
D	Pipe Diameter	(m)
e	Orifice edge thickness	(m)
E	Plate thickness	(m)
k	Turbulence kinetic energy	(m^2/s^2)
m	Mass flowrate	(kg/s)
p	Static Pressure	(Pa)
r	Radial ordinate / Orifice edge-radius	(m)
R	Pipe radius	(m)
Re_D	Pipe Reynolds number	
u	Axial velocity	(m/s)
U	Freestream axial velocity	(m/s)
β	Diameter ratio (= d/D)	(m/s)
ε	Dissipation of k	(m^2/s^3)
μ	Dynamic viscosity	(kg/m.s)
ρ	Density	(kg/m^3)
$\Delta\varpi$	Loss	(Pa)

1 INTRODUCTION

Orifice plates are normally made to a certain thickness to avoid sudden gas surges from buckling the plate and causing it to become lodged in its carrier. However, the length of the constant bore downstream of the square edge should always be less than a specified length (5mm for a 10-inch pipe) to prevent the flow streamlines which have separated from the plate at the square edge from reattaching. In practice this means that the plates must be made with a bevel on the downstream edge of the orifice.

In fiscal applications orifice plates are regularly removed and inspected to ensure that the plate has not become damaged. Through this practice it becomes possible that an orifice plate is installed in reverse orientation with the square-edge of the plate facing downstream. This significantly alters the discharge coefficient of the device, causing a measurement error if the value that is used to calculate the flowrate is unaltered. In some cases reversed plates can go undetected for as much as a year between routine inspections, resulting in a large quantity of gas being mismeasured.

In the case of an identified measurement error it is normal practice that the figures are recalculated and agreed between the relevant parties with reference to the appropriate standards. However in the case of a reversed orifice plate the standards and references are deficient. This paper describes the results of work carried out by NEL to allow mismeasurements to be reconciled in a specific instance of an orifice plate being reversed accidentally.

2 BACKGROUND

Phillips Petroleum Company United Kingdom Limited (Phillips) is the operator of the Judy platform in the UKCS. Gas is exported from Judy via the BP-operated CATS pipeline and is metered using a 4 stream orifice plate station. During a short period in February 2000 a single plate was inadvertently installed back to front for a period of 11 days. The orifice plates have 12-inch nominal bore with a diameter ratio of approximately 0.6 and a 45-degree chamfer on the trailing edge. The volume of gas passed through the metering stream was reported to be approximately 20,000,000 standard cubic meters. It was suspected that a significant mismeasurement had occurred.

The system in question has four metering streams and is represented schematically in Figure 1. The dotted line represents a change of plane from horizontal to vertical (i.e. a 90-degree bend). Streams 1, 2, and 4 were in use in the period of interest. The orifice that was reversed was in Stream 4. Phillips staff made an initial estimate of the mismeasurement by looking at the ratio of reported flows before, during and after the event. It appeared that by increasing the reported flow during the mismeasurement by approximately 2.8 %, the ratio of steams 1 & 4 and streams 2 & 4 would be consistent with the reported flows before and after.

This simple analysis appears effective at a first glance. However, it neglects the fact that the losses in stream 4 are changed when the plate is reversed and this will change the balance of flows. In this case the bevel facing upstream will reduce the losses and hence increase the flow through stream 4 relative to streams 1 & 2.

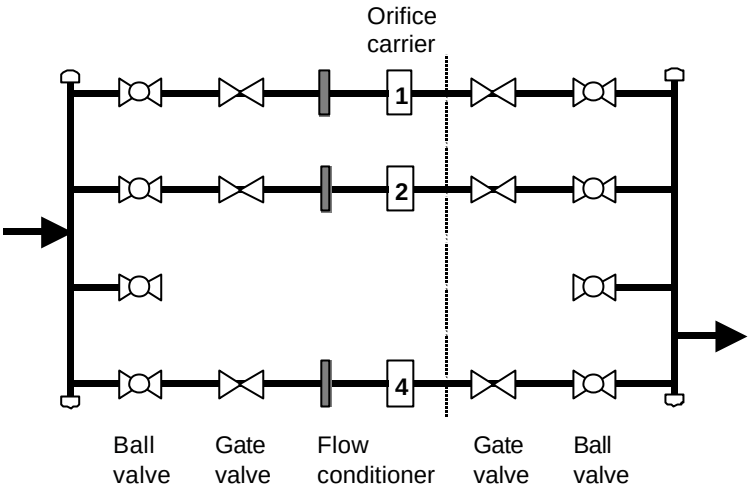

Figure 1 A Schematic of the Orifice Metering System

Prior to this instance NEL had undertaken a study for another client who had experienced a similar problem. During this study NEL established analysis methods by which the magnitude and direction of error could be determined for a given case. In discussion of the Judy case it was realised that the initial estimate of the mismeasurement by Phillips was probably far too low. Phillips therefore initiated a study at NEL in order to determine the magnitude of the mismeasurement for this case.

Figure 2 below shows the edge of the Judy orifice plate. Further dimensional details and application conditions are given below.

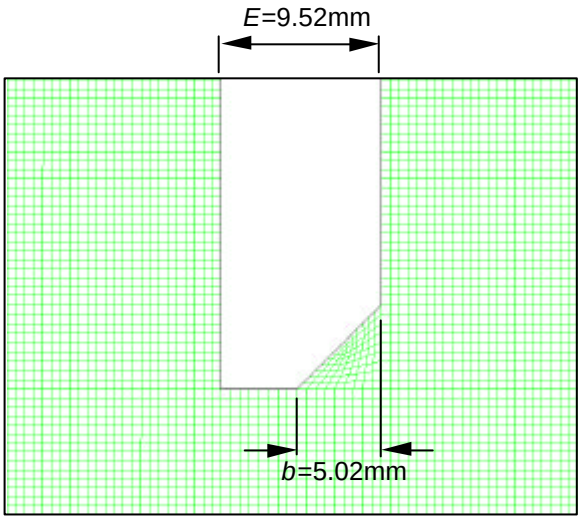

Figure 2 The edge of the Judy Orifice Plate (CFD grid)

Plate and pipe dimensions:

D	=	259.91 mm
d	=	150.80 mm
$\beta=d/D$	=	0.5802
E	=	9.52 mm
e	=	4.5 mm
Bevel angle	=	45°
Flange Taps		

Fluid conditions:

ρ	=	155.489 kg/m^3
μ	=	1.2×10^{-5} kg/m-s
Re_D	=	12.08×10^6
Line temperature	=	53°C
Line pressure	=	159.5 bar g

The discharge coefficient used in normal application, given by the Stolz equation in ISO 5167-1:1991 [1] is C = 0.60408 at these conditions with a differential pressure of 214 mbar. The average upstream velocity is approximately 3.6 m/s.

3 PUBLISHED LITERATURE

The published literature relating to the discharge coefficients of reversed orifice plates has notable deficiencies when considered for general application. In most papers the orifice plates are not fully described: some papers do not give the bevel angle, and the size of the bevel is rarely stated.

ISO/TR 12767 [2] Section 8.6.2 provides information on the variation of discharge coefficient with bevel size. However, as no orifice diameter is given the data cannot be used to determine the magnitude of error in a specific case of interest. ISO/TR 15377 [3] Section 6.1 describes the 'conical entrance' orifice, which is considered to have a constant discharge coefficient of 0.734. However it is recognised that the conical entrance orifice is not sufficiently representative of the reversed squared-edged orifice plates to be of much use. In SPE note 22867 [4] the author describes the results of a number of tests with air at low Reynolds numbers. The tests were carried out for various β, but neither bevel angle or bevel size is given in the paper. When consulted, the author stated that he believed that the bevel angle was 30° to the face of the plate.

Witte [5] has published a paper on the effect of reversing orifice plates in a 250 mm (10-inch) pipe in gas at 60 bar g. The plates had thickness, E, of 6.35 mm (¼ inch) with 45º bevel. The edge thickness, e, was 4.76 mm (3/16 inch), although this is not stated in the paper. Witte carried out the work at the Gas Research Institute Metering Research Facility at Southwest Research Institute. Morrow [6] has reanalysed Witte's data and shown that the effect of reversed flow is largely a function of orifice diameter. Morrow has also measured the effect of reversing a series of plates in a 100 mm (4-inch) line; these plates had a bevel angle of 45°, a plate thickness, E, of 3.18 mm (1/8 inch) and an edge thickness, e, of 1.59 mm (1/16 inch).

The data of Witte and Morrow are by far the most useful data in this case and are discussed later in the paper.

4 EVALUATION OF THE MISMEASUREMENT USING CFD

4.1 Introduction

In order to evaluate the change in the discharge coefficient for the specific case in question, a series of simulations were carried out using computational fluid dynamics (CFD). The commercial CFD package Fluent^{TM} (Version 5.3) was used to solve the flow. The orifice plate was modelled in both the forward and reverse orientation, so that comparison between the results of the two directions could be carried out. The flow was assumed steady, turbulent and incompressible throughout the computational domain. The realisable k-ε model [7] was used to compute the turbulence, as this model was seen to perform well in predicting the flow through an axisymmetric orifice plate during previous work at NEL.

In addition to the specific case of the Judy plate, a number of additional runs were computed, primarily to assess the effect of altering the plate dimensions and Reynolds number on the shift in *C*. The purpose of changing dimensions (such as bevel length and β) was twofold:

- To attempt to explain effects observed in available test results
- To assess how effective the model is in picking up subtle changes in plate geometry

4.2 Methodology

Figure 3 illustrates the boundaries of the computational domain. An axis of rotational symmetry was used (at $r = 0$); this assumes that the flow through the plate is steady and axisymmetric, thus reducing the number of cells required (and hence reducing computational time). The overall length of the domain in the axial direction is 6D. Flow is from left to right and the inlet and outlet boundaries are set 3D upstream and downstream of the plate accordingly. For the reverse direction, these boundaries were simply swapped so that the flow went from right to left. The boundary conditions used assumed fully-developed flow at the inlet and hydraulically smooth pipe walls.

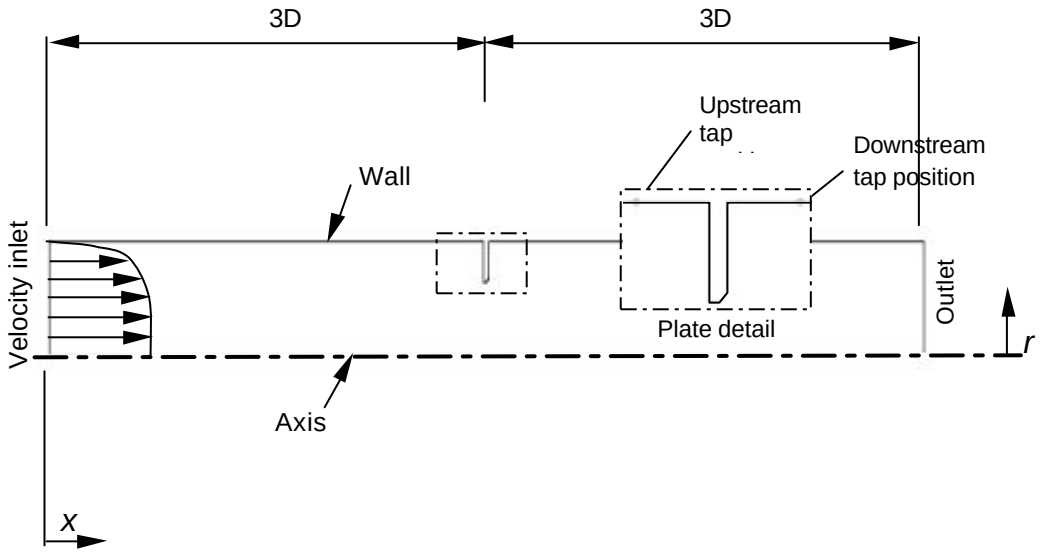

Figure 3 Grid Domain for Orifice Computations (Forward Flow Direction Shown)

Turbulence Model

The flow through the orifice plate will be turbulent; therefore, an additional set of equations (commonly referred to as the turbulence model) must be solved to model these effects. There are a vast number of turbulence models available, of varying complexity and applicability, the most popular (and widely available) being the two-equation k-ε models. The realisable k-ε model was chosen, owing to its reported improvement in modelling axisymmetric jets and separated flows.

All k-ε models incorporate two separate transport equations for the turbulence properties, one for k (the kinetic energy of the turbulence, in m^2/s^2) and the other for ε (the turbulence dissipation, in m^2/s^3). The realisable k-ε model is a relatively new addition to the fold and, owing to improvements in how ε and the turbulent viscosity are computed, is expected to be better suited for solving flows incorporating axisymmetric jets and separation, both of which are present in flows through orifice plates.

Computational Grid

In order for the CFD package to integrate the fluid properties (such as pressure, velocity and turbulence), the domain must be broken up into cells, concentrated where the gradients in the properties are expected to be high. A fine mesh, using just over 130,000 cells, was employed to represent the orifice geometry. Figure 2 (previous) shows the grid detail around the orifice edge. A region spanning the pipe cross-section, and extending a pipe diameter, *D*, upstream and downstream of the plate, was filled with square cells; this ensured that the cell structure surrounding the plate was the same for both the forward and reverse orientations. The size of these square cells was 1.05mm, giving 8 cells along the orifice-edge and 14 along the bevel. Outside the square-celled region, the grid was expanded to the inlet and outlet planes to optimise the cell-count. The grid around the 45° bevel is unstructured, using a special 'tri-primitive' scheme to minimise cell-skewness; this also facilitated the alignment of the adjacent cells with the bevel-wall. Elsewhere, the grid is set out in a structured array; this is recommended so as to minimise numerical errors.

5.3 Analysis of the CFD Result for the Judy Orifice Plate

Figure 4 shows combined velocity/pressure plots from the CFD analysis, depicting the flow around the tip of the orifice plate in the forward and reverse orientations respectively. With the plate facing forward (Figure 4a), the flow moving down the upstream wall is forced to turn rather abruptly by the sharp, leading edge of the plate. In the reverse case (Figure 4b), the flow is turned through 45° by virtue of the bevel, which acts as a kind of nozzle; there is some evidence of a separation bubble along the bevel-edge, which would appear physically realistic. In this case, the resulting jet is at a more acute angle than the forward case, giving a different separation region downstream of the plate; this is discussed below.

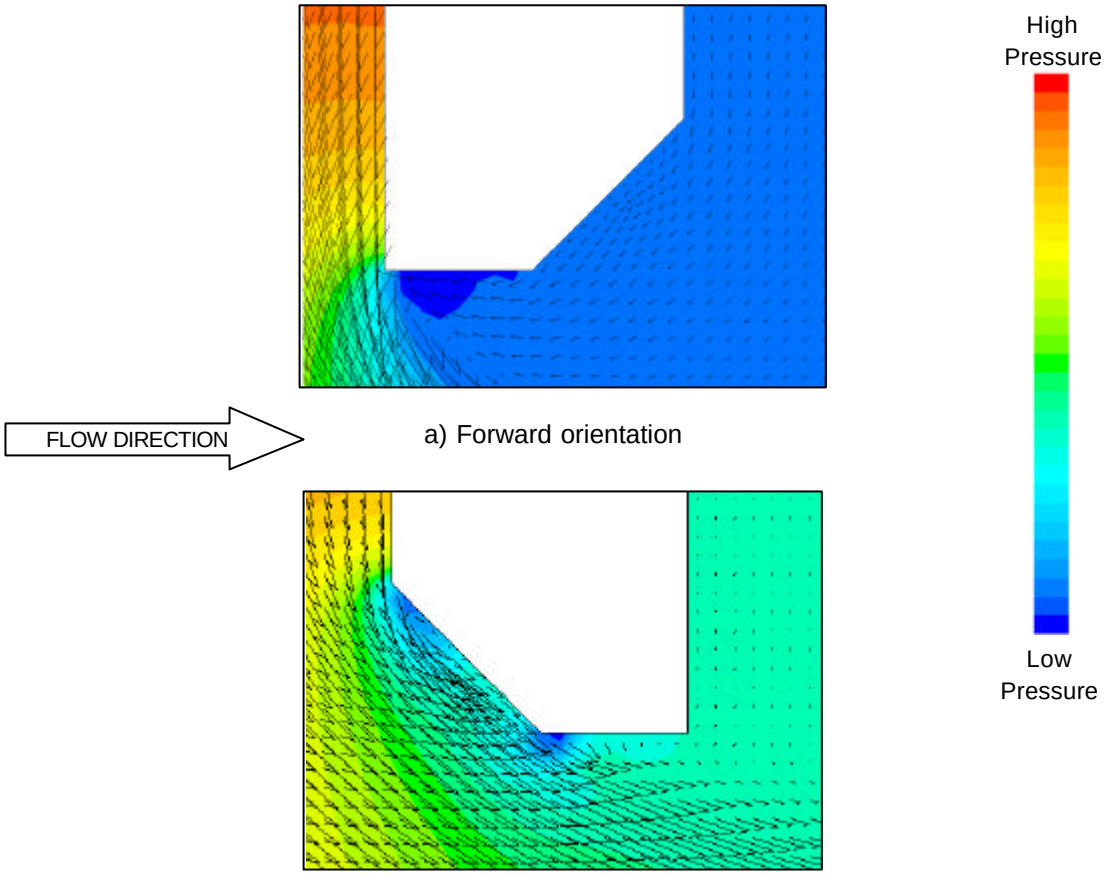

Figure 4 Separation around the Plate Edge for the Two Orientations

Figure 5 illustrates the pressure variation along the upstream and downstream walls of the Judy orifice plate; the pressure is referred to that on the wall at the upstream tap position, given as p-p_{ups} (Pa). The downstream profiles for the plate in the forward and reverse orientations are shown on the same plot (the pressure collapses onto a universal curve upstream of the plate). The shape of the pressure profiles in the two orientations is similar; a region of fairly constant pressure occurs just downstream of the plate (within which the downstream pressure tap is located, indicated by the broken line); within this region the pressure declines slowly to a minimum; this is followed by a recovery towards the exit plane. Included on the chart is the effect of adding an extra 2D onto the downstream; this made no difference to the pressure, indicating that 3D is a sufficient downstream length with which to model the orifice correctly.

Indicated on the two charts is the pressure drop, Δp, of approximately 21,000 Pa, for the plate in the forward direction. Using the Stolz equation, ISO 5167-1 quotes the uncertainty in C as $\pm$ 0.6%, for β = 0.6; the corresponding uncertainty in Δp across the plate would therefore be $\sim 2 \times 0.6 = \pm 1.2\%$, as indicated by the error bars on Figure 5. The CFD result for the plate in the forward orientation is seen to lie just below this band. It is seen from Figure 5 that the pressure differential is not as high in the reverse orientation (being some 15,000 Pa in magnitude); this means that the actual value of C will be higher than that given for the plate in the forward orientation. The shift in the discharge coefficient between the reverse and forward direction is given as

$$\%\frac{C_{actual} - C_{Stolz}}{C_{Stolz}} \equiv \frac{(C_{reverse} - C_{forward})_{CFD}}{(C_{forward})_{CFD}} \times 100$$

This value is always positive, indicating that the actual C value is larger than the one given by the Stolz equation.

The discharge coefficient predicted by the CFD is evaluated using the standard equation for an incompressible flow. In this instance, the 'actual' mass flow rate is that set by the inlet boundary condition, where $\dot{m} = \rho A U$

$$C = \frac{\dot{m}\sqrt{1 - b^4}}{A_2\sqrt{2r\Delta p}}$$

Using the above equations, the resulting shift in C, caused by reversal of the Judy plate was calculated to be +21.67%.

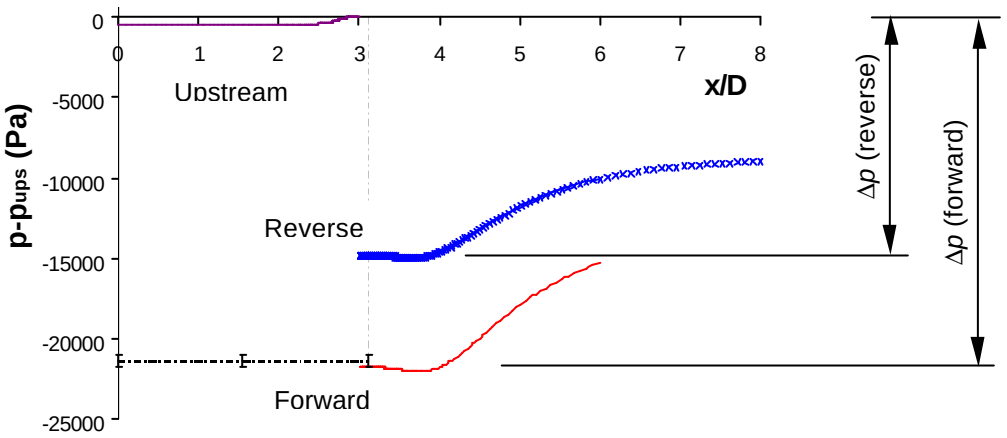

Figure 5 Static Pressure Upstream and Downstream of the Plate [†].

[†] Referred to intlet tap pressure. Error bars refer to ± 1.2% uncertainty in Δp (0.6% in C), as given by the Stolz equation in ISO 5167-1, for this plate-configuration.

Figure 6 shows the trace of zero axial velocity (and, hence, the development of the jet) for both plate-orientations, superimposed onto one plot. The separation region is longer in the forward orientation than the reverse, owing to the angle of incidence of the jets being different. The diameter of the jet in the reverse case is visibly wider and the corresponding pressure loss across the plate is smaller. It is this through this mechanism that the value of *C* is increased.

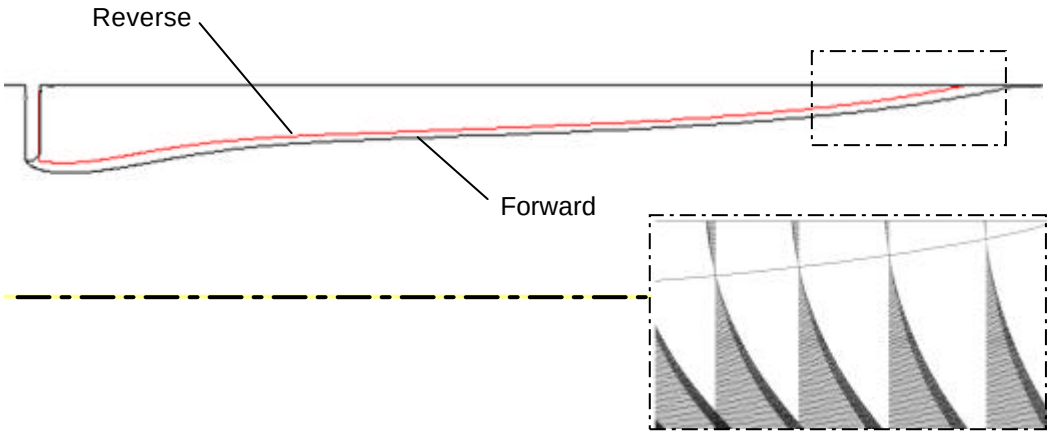

Figure 6 A Comparison of Separation Streamlines in Forward and Reverse Orientations (inset - predicted velocity vectors at reattachment for the forward case)

5 COMPARISON OF THE CFD RESULT WITH EXPERIMENTAL DATA

From analysis of discharge coefficients for orifice plates with rounded upstream edges it appears that to treat a bevel as similar to a rounded edge is satisfactory. The important parameters, therefore, are the width of the bevel and the orifice diameter. Diameter ratio and pipe diameter are less important. So to determine the change in discharge coefficient, the data of Witte and Morrow seem most appropriate in this case. Their data is replotted in Figure 7 as a function of the normalised bevel width, *b*, which is defined as *E* – *e*. Included on the chart is the data point from the Judy CFD analysis.

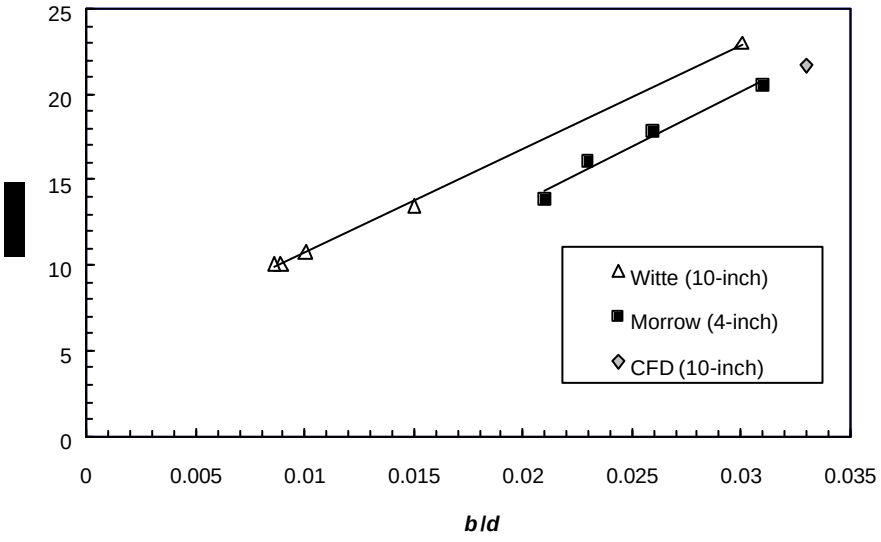

Figure 7 Percentage Shift in C as a function of bevel-to-orifice diameter-ratio, *b*/*d*

It appears, at first glance, that the shift in C is linear with b/d, with the two data sets being segregated by D. If Witte's data are fitted linearly then at the Judy value of b/d = 0.0333 the discharge coefficient would increase by 24.0 per cent. If Morrow's data are fitted linearly then at b/d = 0.0333, the discharge coefficient would increase by 22.0 per cent.

If the difference between Morrow's and Witte's results were thought to be due to pipe diameter, the change in discharge coefficient due to the reversal of the Judy plate would be 24.2 per cent. However, the CFD data point lies closer to Morrow's data than Witte's, despite Witte's plate being of similar bore to the Judy plate. It appears reasonable therefore, that the pipe diameter may not be the parameter responsible for the offset between Morrow's and Witte's lines.

Both sets of experimental data were generated with a fixed bevel length, b, whilst d (and hence β) were varied to give the ranges of b/d plotted. Therefore, the data cannot show if similar trends would result from tests with b altered independently of d. One possibility is that the difference between the two sets is due to the different values of b/E (which is 0.24 in the case of Witte's data, 0.5 in the case of Morrow's data and 0.53 in the case of the Judy plate). On this basis a reasonable estimate of the change in discharge coefficient due to the reversal of the Judy plate is 21.8 per cent.

The remainder of the CFD work was aimed at determining the effect of changing the plate dimensions on the shift in C, with a view to understanding the behaviour of the flow in the reverse orientation. This, together with an analysis of the effect of Reynolds number, is investigated in the next section.

6 THE EFFECT OF PLATE DIMENSIONS AND REYNOLDS NUMBER

It is necessary to consider the plate dimensions used by Witte, Morrow, and in the current case, in more depth. Table 1 details the salient dimensions of the plates used in each case. An important parameter is the ratio of the bevel length to the plate thickness, b/E. This parameter is similar for the Judy and Morrow's plates, whilst substantially smaller in Witte's case, perhaps explaining why the CFD point is closer to Morrow's line than Witte's. Also apparent from Witte's report is that the value of b/d closest to the Judy case was for the plate with the lowest diameter ratio (β=0.208); there is also a lack of data available at the upper end of b/d to substantiate a linear trend with b/d. Another parameter worth considering is the Reynolds number; all of Witte's tests for $\beta < 0.4$ were for $Re_D < 10^6$ and, for the data point closest to the Judy case, the range tested was $2.5\times10^5 < Re_D < 7.5\times10^5$ which is much lower than the Judy case.

Table 1 Salient Plate Dimensions for the Three Cases Under Analysis

Name	Re_D	$\beta=d/D$	b/d	b/E	bevel
Witte	2.5×10^5 - 12.8×10^6	0.208 - 0.728	0.009 - 0.030	0.25	45°
Morrow	Not stated	0.5 - 0.75	0.021 - 0.031	0.5	45°
Judy	12.08×10^6	0.58	0.033	0.53	45°

A number of additional simulations were computed, to assess the effect of altering the plate dimensions, and Reynolds number, on the shift in C. In all cases, the models were run in the forward direction, as well as the reverse, but it was found that the behaviour of C in the forward direction was less dependent on the plate dimensions than in the reverse direction.

Examining the b/d parameter

There are two ways of altering b/d; the first method is to change b, whilst fixing d, the second is to change d (and hence β), whilst fixing b. The latter method simply replicates what Witte and Morrow did experimentally, whilst the first should be more revealing as to the bevel-influence. It appears prudent to model the plate with a b/d value falling within the range of Witte and Morrow. In the first case, b was set to 3 mm, to give b/d=0.02. To attain a lower b/d using the second method, the diameter ratio had to be increased. If β is taken to the upper limit (specified in ISO 5167-1 as β=0.75), this gives a corresponding value of b/d=0.0256, provided the geometry of the plate-edge remains unchanged.

Figure 8 details the grid surrounding the plate for the b=3 mm case; the parameter e is increased accordingly to e=6.52 mm, to accommodate the change in bevel length. The grid-configuration and mesh density are identical to what they were previously, except in close proximity to the plate. The same 'tri-primitive' meshing scheme is used around the bevel and although there are fewer cells covering the length of the bevel, the number of cells per unit length remains unchanged. The grid structure for the β=0.75 case (not shown) was identical to the β=0.58 case, except that the orifice diameter was increased to 195 mm, with extra cells duly added to fill the wider orifice-area.

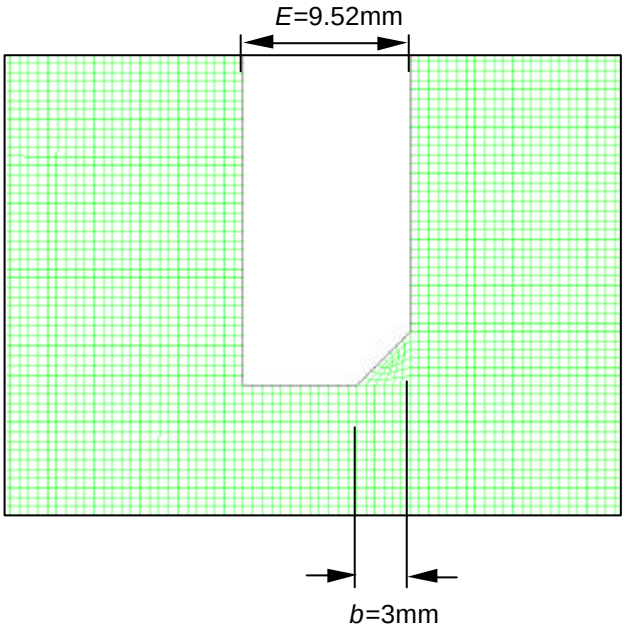

Figure 8 Detail of Mesh at the Edge of the Plate with Reduced Bevel.

Examining the b/E parameter

Another variation that can be introduced is to reduce the length of the orifice land, e, whilst fixing b; this means that the overall plate thickness, E, must also be reduced. Figure 9 details the two grids used for this case. The first test was to reduce the land-length to 2 mm, giving b/E=0.72 (Figure 9a), whilst the second test was to remove the land entirely, giving b/E=1 (Figure 9b). It is noted that the first test is within the geometrical limits set by ISO 5167-1 (which designates a lower limit on e of 1.3 mm for a 10-inch pipe), whilst the second violates this limit, with e=0. It is also noted that the e=0 case would not be a practical design, owing to difficulties in manufacture and possible damage to the sharp-edge when in use.

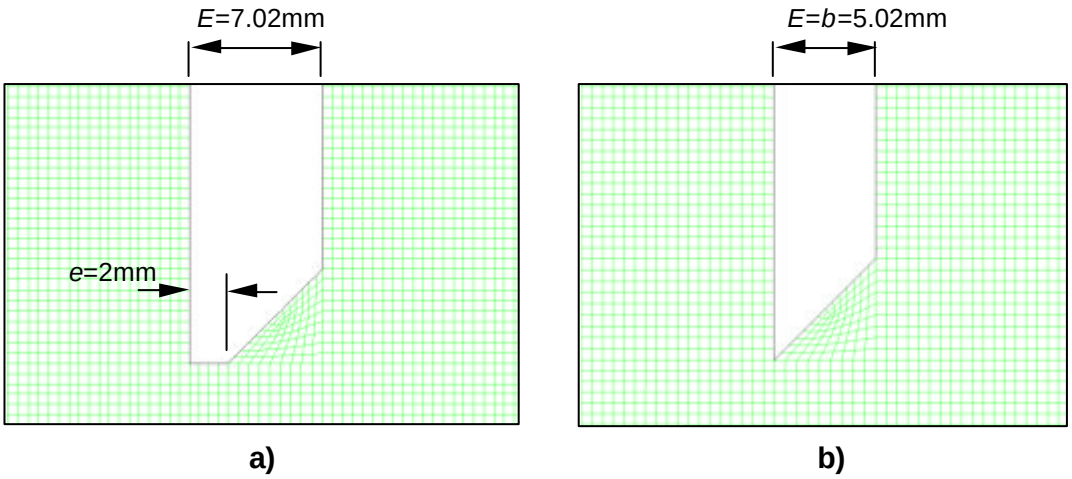

Figure 9 Detail of mesh surrounding the Judy plate with reduced orifice-land: a) e=2mm, b/E=0.72. b) e=0mm, b/E=1

Reynolds number influence

It is clear from Witte's paper that, despite the author claiming there is no Reynolds number influence on his data, the results at the lower end of Re_D, corresponding to $\beta < 0.6$, show considerable scatter. The spread in the data increases with decrease in Re_D, with step changes in the results occurring below $\beta < 0.624$, presumably owing to Reynolds number change between each set of points plotted for each specific β. It is not stated whether it was the Reynolds number that Witte changed between each of the sets, or some other parameter, but the latter seems most likely.

To investigate if Reynolds number has any influence the shift in C, the CFD was again employed for the geometry specific to the Judy plate (i.e. β=0.58, b/d=0.033, 10-inch pipe). The Reynolds number was reduced to 2×10^6, and the model was run in both orientations. The grid used was identical to that for the original computations. The resulting shift in C was 21.65%, which is very similar to the result for $Re_D=12.08\times10^6$. We can conclude that there is no significant Re_D effect within this range of Reynolds number.

Results

Figure 10 details combined pressure and velocity plots for the four cases in the reverse orientation, with Figure 10a being the Judy plate. It is seen that reducing the bevel length produces the biggest effect on the pressure, albeit only locally (Figure 10b), the pressure drop at the bevel being larger in this case. Reducing the orifice land from 4.5 to 2 mm does not appear to make a significant difference to the pressure contours around the plate-lip, whilst completely removing the orifice land rids the solution of the suction effect at the jet-separation point, caused by the presence of the land (Figure 10d). The velocity vectors show a progressively cleaner separation from the downstream edge, as e is reduced. Despite the shorter bevel (Figure 10b) making the most change to the flow around the plate-lip, the value of C in both orientations was much the same as for the Judy plate (see Table 2).

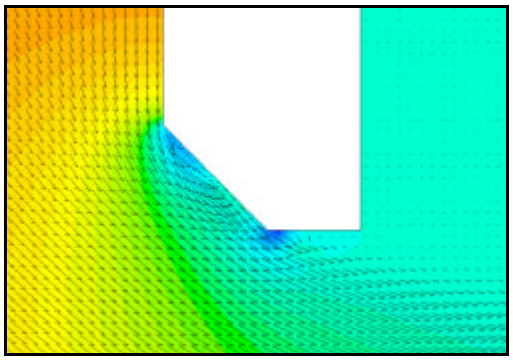

a) Judy Plate (*b*/*d*=0.033, *b*/*E*=0.53)

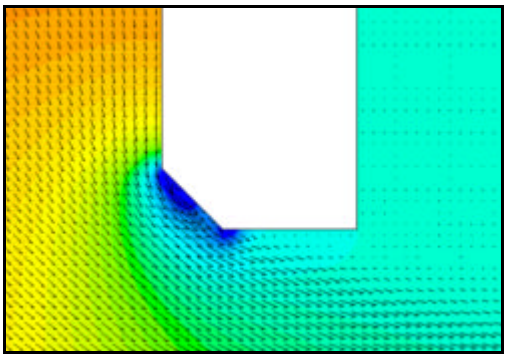

b) Reduced bevel (*b*/*d* =0.02, *b*/*E* =0.32)

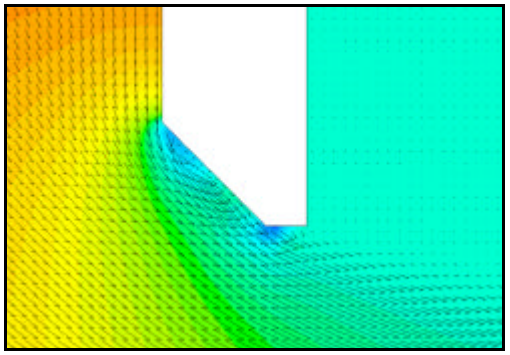

c) Reduced orifice (*b*/*d* =0.033, *b*/*E* =0.7)

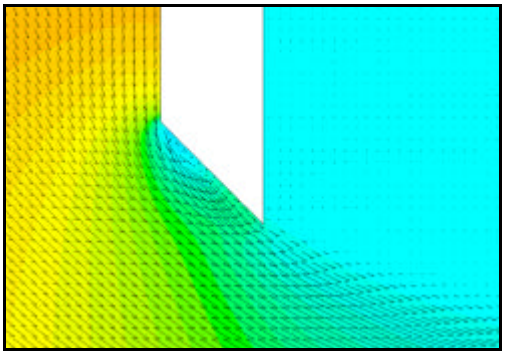

d) No Orifice-land (*b*/*d* =0.033, *b*/*E* =1)

Figure 10 Combined Pressure/Velocity plots for four different plates in reverse orientation

Figure 11 presents the results of all of the computations performed, including the modifications to the plate geometry. All of the data are tabulated in Table 2. As mentioned before, the value of *C* for the forward direction was checked in all cases, but was found to vary by only about 0.5% from the original Judy plate result, for β=0.58. For the β=0.75 case, *C* was about 1% below the limits of the Stolz equation in the forward direction (compared to about 0.2% for the β=0.58 case). Considering the effect of altering *b*/*d* first, it is seen from the chart that the point for *b*/*d* =0.0256 (as achieved by changing β to 0.75) lies on Morrow's line. The second method used for reducing *b*/*d* was to decrease the bevel length from 5.02mm to 3mm, whilst fixing β=0.58. This point can be seen to lie somewhat above the test data, with the magnitude of the error being, in fact, almost identical to that from the first simulation (i.e. for *b*/*d* =0.033, *b*/*E*=0.53).

The CFD predicts a markedly different influence owing to the *b*/*d* parameter, depending on whether it *b* or *d* that is changed; however, it is noted that, in changing *b* with a fixed plate thickness *E*, the ratio *b*/*E* became smaller, at 0.3.

The influence of altering the ratio *b*/*E* was evaluated by reducing the orifice land-length, *e*. The effect of making these modifications is depicted by the three points aligned at *b*/*d*=0.033, to the right of the chart. The CFD predicts that an increase in *b*/*E* results in a decrease in the error in *C*; this appears to substantiate the premise that Witte's and Morrow's lines are separated due to the influence of this parameter.

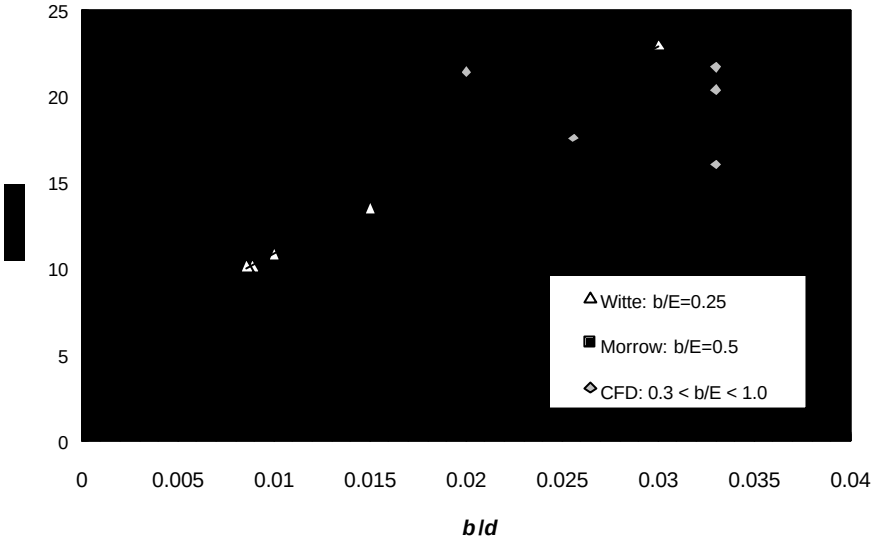

Figure 11 Effect of Various Geometry Modifications on the Resulting Error in *C* (Note: β=0.58, unless otherwise stated)

The unexplained result is still that produced by reducing the bevel size to 3mm, which lies above all the results, despite having a *b*/*E* value that lies between Witte and Morrow's data. There are several possible explanations for this; the first is that the *b*/*E* effect may also be dependent on *b*/*d*, whilst the second is that the CFD is not capable of picking up the bevel effect entirely satisfactorily. It should be noted that there are no experimental data points that can be used to substantially verify or reject this specific result. Without additional test data, for plates with differing *b*/*d* and *b*/*E* ratios, it is difficult to ascertain which effects are dominant.

Table 2 Combined Results of the CFD Computations

Re_D	β=*d*/*D*	*e*	*b*	*b*/*d*	*b*/*E*	C_{Stolz}	$C_{forward}$	$C_{reverse}$	%d*C*/*C*
12.08×10^6	0.5802	4.5	5.02	0.033	0.53	0.6041	0.5990	0.7289	21.67
12.08×10^6	0.5802	4.5	3.02	0.020	0.32	0.6041	0.5990	0.7271	21.38
12.08×10^6	0.5802	2.0	5.02	0.033	0.72	0.6041	0.5974	0.7210	20.36
12.08×10^6	0.5802	0.0	5.02	0.033	1.00	0.6041	0.5957	0.6910	16.00
12.08×10^6	0.7500	4.5	5.02	0.033	0.53	0.5975	0.5875	0.6903	17.50
2.00×10^6	0.5802	4.5	5.02	0.033	0.53	0.6041	0.5994	0.7292	21.65

6 ANALYSIS OF PHILLIPS DAILY REPORT DATA

Phillips supplied daily reports of the data collected before the plate was reversed, during the period it was reversed, and after the correction of the reversal. This information allows evaluation of the change in discharge coefficient based on a loss-balance approach.

When the plate was reversed in stream 4 the differential pressure in stream 4 reduced in comparison with the differential pressure in the other streams. In fact, the flow in stream 4 actually increased, but the discharge coefficient increased and the other losses increased relative to the loss at the orifice plate. To determine the change in discharge coefficient it is necessary to determine the loss in each tube between locations in the 24-inch header near to inlet and outlet. This can be done approximately by reference to Miller [8].

The total loss in each run can be given as:

$$\Delta v = K_{tot} \tfrac{1}{2} \rho U^2 + f_{orifice} \Delta p$$

where K_{tot} is the sum of the loss coefficients for all components excluding the orifice plate and $f_{orifice}$ is given by

$$f_{orifice} = \frac{\sqrt{1 - b^4(1 - C^2)} - Cb^2}{\sqrt{1 - b^4(1 - C^2)} + Cb^2}$$

Table 3 below shows the estimated loss coefficients for each of the components that make up the streams, excluding the orifice plates. It also shows the total loss calculated in each stream using the day-averaged flowrate, density and differential pressure values from a typical report prior to the mismeasurement (16/02/00). Actual values of orifice and pipe diameters were used for each stream.

Table 3 Unbalanced Losses Before Reversal of the Plate (16/02/00)

	Loss Coefficient, K		
	Stream 1	**Stream 2**	**Stream 4**
Junction with Stream 2 inlet	0.01		
Inlet to stream	0.44	0.79	0.44
2 ball valves	0.1	0.1	0.1
2 gate valves	0.3	0.3	0.3
Flow conditioner	1.4	1.4	1.4
Straight pipe	0.77	0.77	0.77
90 bend	0.16	0.16	0.16
Outlet from stream	0.79	0.9	0.79
Junction with Stream 2 outlet	0.2		
K_{tot}	**4.17**	**4.42**	**3.96**
Density (kg/m^3)	152.8	152.73	152.76
Flowrate (m^3/hr)	540.27	533.42	536.81
C	0.6041	0.6041	0.6041
$f_{orifice}$	0.6548	0.6545	0.6535
ΔP (Pa)	13339.4	12989.4	12846.6
Loss (Pa)	**11279**	**11134**	**10746**
% difference from mean	2.04	0.73	-2.78

Since in fact the loss must be the same in each stream it is clear that the actual values of K_{tot} must be different from the estimates. Keeping the sum of the head loss coefficients the same while making all the streams balance gives coefficients of 3.80, 4.28 and 4.47 respectively as given in Table 4.

Table 4 Balanced Losses Before Reversal of the Plate (16/02/00)
(losses equal to the mean of the unbalanced result)

	Stream 1	**Stream 2**	**Stream 4**
K_{tot}	**3.80**	**4.28**	**4.47**
Density (kg/m^3)	152.8	152.73	152.76
Flowrate (m^3/hr)	540.27	533.42	536.81
C	0.6041	0.6041	0.6041
$f_{orifice}$	0.6548	0.6545	0.6535
ΔP (Pa)	13339.4	12989.4	12846.6
Loss (Pa)	**11051**	**11051**	**11051**
% difference from mean	0.00	0.00	0.00

Keeping the same loss coefficients we can now enter the day-averaged flowrate, density and differential pressure values from a typical report during the mismeasurement (20/02/00). This results in losses of 10495 and 10466 Pa for streams 1 and 2 respectively and would result in a loss of 9899 Pa for stream 4 if C were unchanged. However, as the losses should balance and the orifice plate is the only part of the system that has been changed, the discharge coefficient must be increased in stream 4 which increases U and reduces $f_{orifice}$. To make the loss in stream 4 equal to average of the other two streams requires that C be increased to 0.7540. This is an increase in C of 24.8 per cent. The result of balancing the reversed orifice flow is presented in Table 5. Note that the flowrate for stream 4 was reported to be 506.94 m^3/hr in the report dated 20/02/00. This has been multiplied by the ratio of the revised discharge coefficient to the assumed discharge coefficient to give the actual flowrate for the loss calculation.

Table 5 Balanced Losses Following Reversal of the Plate (20/02/00)
(K_{tot} from Table 4)

	Stream 1	**Stream 2**	**Stream 4**
K_{tot}	**3.80**	**4.28**	**4.47**
Density (kg/m^3)	152.95	152.86	152.86
Flowrate (m^3/hr)	525.20	517.92	**632.73**
C	0.6041	0.6041	**0.7540**
$f_{orifice}$	0.6548	0.6545	**0.5892**
ΔP (Pa)	12678.3	12315.8	11524.2
Loss (Pa)	**10495**	**10466**	**10480**
% difference from mean	0.14	-0.14	0.00

This result is sensitive to the method that has been used to achieving balance. We could decide that, rather than adjusting the values of K_{tot} to keep the average loss constant; it would be better to assume that there were additional losses within the system. Then balance is achieved by keeping the original estimate of K_{tot} in stream 1 and increasing K_{tot} in streams 2 and 4 so that the losses using the 16/02/00 data equal 11279 Pa in each stream. The K_{tot} value for streams 2 and 4 then become 4.66 and 4.86 respectively. To achieve balance using the 20/02/00 data the value of C required is 0.7355, an increase of 21.7 per cent. This result is based on an increase in K_{tot} for Stream 4 of 0.9. The results obtained are presented in Table 6.

Table 6 Balanced Losses Following Reversal of the Plate (20/02/99)
(K_{tot} in streams 2 and 4 increased to achieve balance)

	Stream 1	**Stream 2**	**Stream 4**
$\boldsymbol{K_{tot}}$	**4.17**	**4.66**	**4.86**
Density (kg/m^3)	152.95	152.86	152.86
Flowrate (m^3/hr)	525.20	517.92	**618.46**
C	0.6041	0.6041	**0.7355**
$f_{orifice}$	0.6548	0.6514	**0.5968**
ΔP (Pa)	12678.3	12315.8	11524.2
Loss (Pa)	**10709**	**10679**	**10694**
% difference from mean	0.14	-0.14	0.00

7 OFFSHORE VERIFICATION TESTS

Following presentation and discussion of the NEL results and analysis the interested parties decided that Phillips should conduct a trial offshore to confirm the estimate of the mismeasurement. The plan for these tests agreed was straightforward. On a day when gas production was deemed to be steady data would be logged at fifteen-minute intervals and the orifice would be reversed again.

Data was logged directly from the flow computers and on the Darius data acquisition system. Analysis of the data taken from the flow computers resulted in an estimate of the increase in discharge coefficient of 19.6%.

Figure 12 below shows results taken from the Darius system. This data covers a period of three hours and thirty minutes before the plate was reversed, seven hours while the plate was reversed and five and half hours after it had been returned to its proper installation.

Although the flow is unsteady the drop in reported flowrate is clear as shown by the line representing the average in each period. Subtracting the average 'reversed' flow from the average of the results obtained before and after reversal of the plate gives a difference of 19.85 kSm^3/hr. Using the Stream 4 average of 102.43 kSm^3/hr this difference can be equated to an increase in discharge coefficient of 19.4%. The difference in the average flowrate before and after the reversal of the plate was approximately 2 kSm^3/hr or 2 % of the stream 4 flowrate.

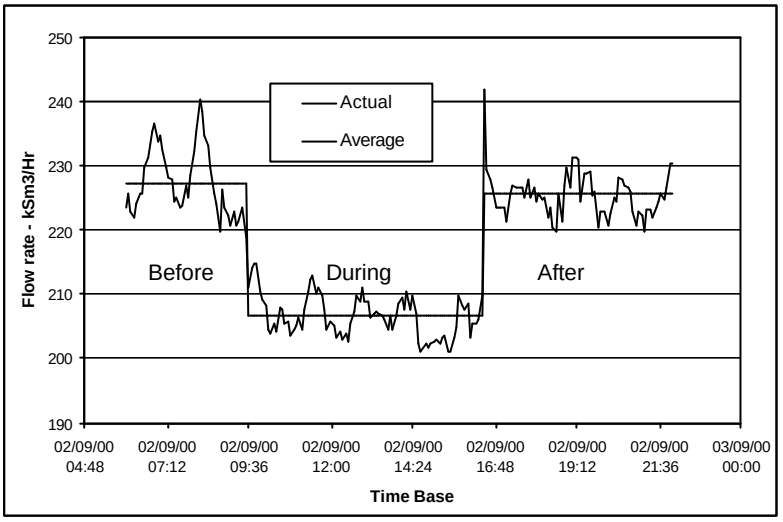

Figure 12 Reported Flow Through Streams 2 & 4 during Reverse Orifice Tests

By aligning the end of each series of data, a calculation on a point-by-point basis can be carried out. Owing to the fact that the flow is unsteady a large spread of results is expected, as the flowrates-versus-time series are uncorrelated. However, the histogram in Figure 13 shows that 70% of the 108 points calculated lie between 15 and 25 %.

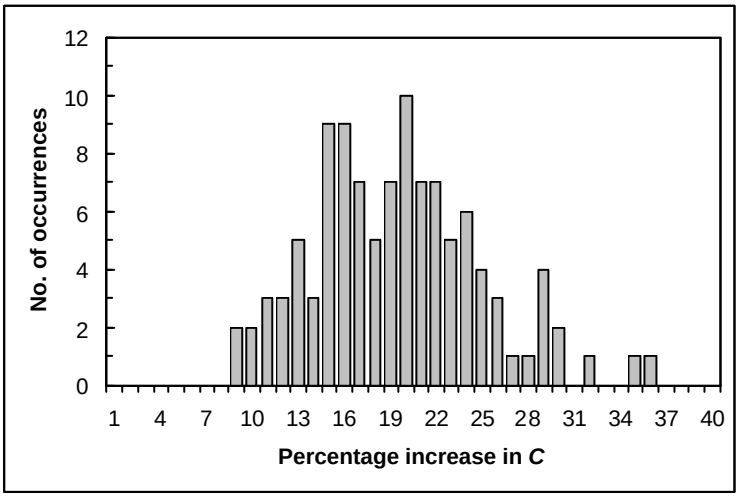

Figure 13 A Histogram of Results Calculated on a Point-by-Point Basis

8 DISCUSSION AND CONCLUSIONS

Reversing an orifice plate that has a beveled trailing edge can cause a mismeasurement of significant magnitude. As the standards are deficient with respect to this problem, alternative methods of evaluating the magnitude of the mismeasurement are required.

A number of methods were applied to determine the increase in the discharge coefficient when one of the orifice plates on Judy was reversed.

A CFD analysis of the Judy plate was been undertaken. Using the realisable k-ε model, with a grid of just over 130,000 cells, the predicted increase in *C* was 21.7%.

Extrapolation from individual sets of experimental data resulted in predicted increases in *C* of 24.0 and 22.0% from the data of Witte and Morrow respectively. Assuming that the difference between the two sets of results is due to differences in pipe diameter the increase would be 24.2%. However, if the difference is assumed to be due to the difference in the ratio of bevel size to plate width then the increase would be 21.8%.

A loss-balance was applied using the before and after flow data from the Judy reporting system. Balancing the losses results in an estimate of the increase in *C* of 24.8% when the sum of the losses is kept constant. If the losses are increased until balance was achieved, the increase in *C* is 21.7%.

Data from offshore verification trials indicated that the increase in *C* was approximately 19.4%.

Taking the analysis methods together, an increase of 22% is a good estimate of the change in discharge coefficient due to the reversal of the Judy plate. Hence any flow derived values (e.g. total volume at standard conditions) from the period during which the plate was reversed could be multiplied by a correction factor of 1.22 as a straightforward way to account for the mismeasurement.

Evaluation of the uncertainty in this final estimate is not trivial. Estimates of uncertainty could be made for each of the analysis methods and then combined appropriately. Taking a pragmatic approach it is probably more useful to accept a value of 3%, which will bring all of the results within the uncertainty band as illustrated in Figure 3.

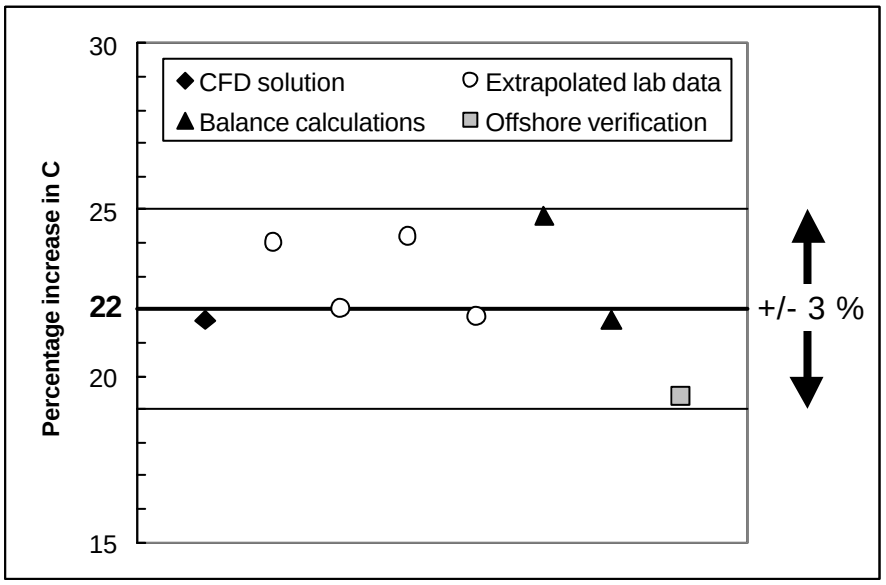

Figure 14 A Summary of the Results using Various Methods

The CFD was able to reproduce the effect of lowering the b/d ratio by increasing d (hence β) whilst keeping b fixed. However, reducing b with d fixed did not reproduce the same effect. The CFD data does indicate an effect from altering the ratio of bevel length to plate thickness, b/E, and this effect ties in qualitatively with the test data of Witte and Morrow, which appear separated owing to the b/E parameter.

As the experimental data does not contain sufficient information to verify fully the CFD predictions a complete picture considering the effects of all of the variables is not yet available. It follows that further work is required before a general model can be developed to allow calculation of the change in discharge coefficient for a given plate geometry. Further CFD simulations may improve our understanding but there is also a clear need for more laboratory data from a wider range of plates.

Additional experimental data may become available in future from laboratories such as NEL and SwRI. It is hoped that analysis of such data will begin to close the gaps in our knowledge of discharge coefficients for reversed orifice plates.

ACKNOWLEDGEMENT

The authors would like to thank Tom Morrow at Southwest Research Institute for his help and co-operation in providing the essential laboratory data.

REFERENCES

[1] INTERNATIONAL ORGANIZATION FOR STANDARDIZATION. Measurement of fluid flow by means of pressure differential devices. Part 1: Orifice plates, nozzles and Venturi tubes inserted in circular cross-section conduits running full. ISO 5167-1: 1991. Amendment 1 was published in 1998.

[2] INTERNATIONAL ORGANIZATION FOR STANDARDIZATION. Measurement of fluid flow by means of pressure-differential devices - Guidelines to the effect of departure from the specifications and operating conditions given in ISO 5167-1. ISO/TR 12767: 1998.

[3] INTERNATIONAL ORGANIZATION FOR STANDARDIZATION. Measurement of fluid flow by means of pressure-differential devices - Guidelines for specification of nozzles and orifice plates beyond the scope of ISO 5167-1. ISO/TR 15377: 1998.

[4] TING, V. C. Effects of non-standard operating conditions on the accuracy of orifice meters. SPE 22867. Society of Petroleum Engineers, 1991.

[5] WITTE, J. N. Orifice meter error with reversed beveled plates. In Proc. AGA Operating Conference, Nashville, Tennessee. Paper 97-OP-062. May 1997.

[6] MORROW, T. B. Private Communication. San Antonio, Texas: GRI MRF, February 2000.

[7] SHIH, T-H., LIOU, W. W., SHABBIR, A., and ZHU, J. A New k-e Eddy-Viscosity Model for High Reynolds Number Turbulent Flows - Model Development and Validation. Computers Fluids, 24(3):227-238, 1995.

[8] MILLER, D. S. Internal flow systems. Cranfield, Bedfordshire: BHRA Fluid Engineering, 1978.